



# AN INTERNATIONAL COMPARISON OF AC JOSEPHSON VOLTAGE STANDARDS BETWEEN NRC, CANADA AND VSL, THE NETHERLANDS

Piotr S. Filipiński<sup>1</sup>, Helko van den Brom<sup>2</sup>, Ernest Houtzager<sup>2</sup>

<sup>1</sup> National Research Council, Ottawa, Canada, Peter.Filipski@nrc-cnrc.gc.ca

<sup>2</sup> VSL Dutch Metrology Institute, Delft, The Netherlands, hvdbrom@vsl.nl

**Abstract:** The paper presents results of an international comparison of two quantum AC Josephson Voltage Standards based on pulse-driven Josephson arrays. The two systems differ in several hardware and software characteristics as well as in the level of automation, features which can influence the accuracy of transferring the quantum-standard voltage value to a calibrated instrument. The comparison was conducted at 100 mV, 20 mV and 12 mV, at frequencies between 2.5 kHz and 100 kHz. An electronically-aided thermal transfer standard was used as a travelling standard. At the most accurate voltage and frequency point, 100 mV at 2.5 kHz, both laboratories agreed to better than 1 part in  $10^6$ .

**Key words:** Josephson arrays, signal synthesis, standards, ac voltage standard.

## 1. INTRODUCTION

An AC Josephson Voltage Standard (ACJVS) is an active source of AC voltage generated by a superconducting array of Josephson junctions. Such a voltage source is in principle quantum-accurate; the generated AC voltage can be calculated solely from the number of junctions in the array, the frequency of microwave irradiation and fundamental constants. In practice, however, the accuracy of such standard is limited by residual parameters of the array, and the instrumentation errors. The transfer of the standard AC voltage value to a secondary standard is also degraded by parasitic parameters of relatively long leads (over 1 m) between the reference plane of the quantum accurate source, immersed in the liquid helium, and the room-temperature secondary standard.

Two types of Josephson junctions (JJ) arrays are employed to generate AC voltage: programmable arrays to generate a step-wise approximation of a sinewave, and pulse-driven arrays, to generate a sinewave as a fundamental component of a sigma-delta modulated pulse train. The former approach is more suited for the generation of voltages of a relatively high value, up to 10 V, but at frequencies not significantly exceeding the power frequency, 50/60 Hz. The latter approach, developed by NIST [1], has a much wider frequency limit, between 1 kHz and 1 MHz, but at a lower voltage. NIST state of the art arrays can generate up to 300 mV rms voltage, when two arrays are connected in series, [2], [3], [4].

The AC Josephson Voltage Standards established at NRC and VSL are based on NIST pulse-driven arrays. They differ in several hardware and software characteristics and in the level of system automation. These features can potentially influence the accuracy of transferring the standard value to a calibrated instrument. The purpose of the comparison was to investigate if there are differences in calibration results obtained in both laboratories.

## 2. DIFFERENCES BETWEEN THE NRC AND VSL SYSTEMS

The operating principle of the ACJVS has been described in detail previously, e.g. [1], [2], [3]. The superconducting Josephson array, mounted inside a cryoprobe and immersed in 4.2 K liquid helium, is excited by a bipolar current pulse train. In response to this input pulse train, a properly excited and biased array produces a train of output voltage pulses. The time integral of each output pulse is quantized, and can be determined with quantum accuracy from two fundamental constants, Planck's constant  $h$  and the electron charge  $e$ . The average output voltage is proportional to the density of the input pulses, i.e., the pulse repetition rate.

When the density of the input current pulses is modulated by a low frequency sinusoidal waveform, the same low frequency harmonic component will appear in the low frequency spectrum of the array output voltage pulses. The magnitude of this component in the exciting pulses, while known accurately from the theoretical modulation pattern, is modified by the actual generator and the transmission path. However, because the area of the array output pulses is perfectly quantized, the magnitude of the low frequency component in the output pulse train can be exactly *calculated* from the known area of the single pulse, the number of Josephson junctions in the array, and the theoretical modulation pattern. This observation is at the foundation of the AC voltage quantum standard.

Whereas NRC and VSL systems operate on the same principle, and use the same NIST pulse-driven arrays, they are not identical. The main differences between the two systems are illustrated on Figs. 1 and 2.

At the core of the VSL system, shown in Fig.1, is a ternary pulse-code generator (PCG), [5]. It produces DC-coupled positive and negative pulses, each returning to zero. The pulse pattern is calculated in advance of the generation

and loaded in the memory of the PCG through the IEEE-488 interface. The pattern memory length of the PCG is 32 Mbits. The lowest frequency that can be synthesized, by use of the 15.5 GHz clock and the whole memory for a single period pattern, is 477 Hz.

The PCG is followed by a power amplifier with a pass band between 10 MHz and 50 GHz. Its output pulses are applied to the JJ array through a semi-rigid coaxial line. The power amplifier is galvanically isolated from the array by an inner/outer DC block (capacitor). The low frequency component in the exciting pulses spectrum is thus significantly attenuated by the limited passband of the amplifier and the capacitive, rather than DC, connection. Furthermore, the peak values of the pulses applied to the array are modified. When the pulse-train modulation depth, i.e. the ratio of the modulating sinewave amplitude to the pulse amplitude, exceeds approximately 10%, the array will no longer operate properly on its first Shapiro step at every exciting pulse and will not respond in a perfectly calculable way. To restore the pulse train to its original form, compensation current is generated by an additional low frequency arbitrary waveform generator, AWG1 in Fig.1, and re-introduced by a separate path. This generator is synchronized with the PCG, and the phase and amplitude of its output is adjusted to properly compensate the attenuated low frequency component of the pulse train.

The voltage output of the array is connected to the room-temperature output of a cryoprobe through a twisted-pair line made of a copper wire. An instrument under test (IUT), such as a Fluke model 792A thermal transfer standard (TTS) used in this comparison, is connected to this output through an additional length of a coaxial cable.

The operation of the VSL ACJVS is fully automated, [6], and the parameter tuning requires either none or a minimal operator intervention. Two instruments, shown in Fig.1 as an I-V sweeper and a spectrum analyzer, serve as auxiliary tools during the automatic parameter tuning. The spectrum analyzer detects when the proper operating conditions have been reached, that is when the low frequency output spectrum contains only the first harmonic (100 to 120) dB above the noise floor, and no significant higher harmonics. The I-V sweeper generates a disturbance signal at the operating point. The downhill simplex algorithm seeks such a plateau in the parameter settings when the proper operating conditions exist under a maximum disturbance signal.

The NRC system, shown in Fig. 2, reproduces the original NIST system, [2]. The exciting current pulses are generated by combining outputs of two commercial generators, a PCG and a continuous wave generator (CWG). The PCG generates non-return-to-zero two-level pulses, which can only be used to generate a unipolar voltage. However, when its output is combined with the output of a CWG, both positive and negative pulses, necessary for generation of AC voltage, can be created, [7]. To ensure that each exciting pulse will cause the array to operate on its first Shapiro step, the frequency ratio of the outputs, their amplitudes and relative phases have to be properly set.

To obtain the effective 10-GHz pulse train, the PCG is clocked at 10 GHz and its output is combined in a 6 dB

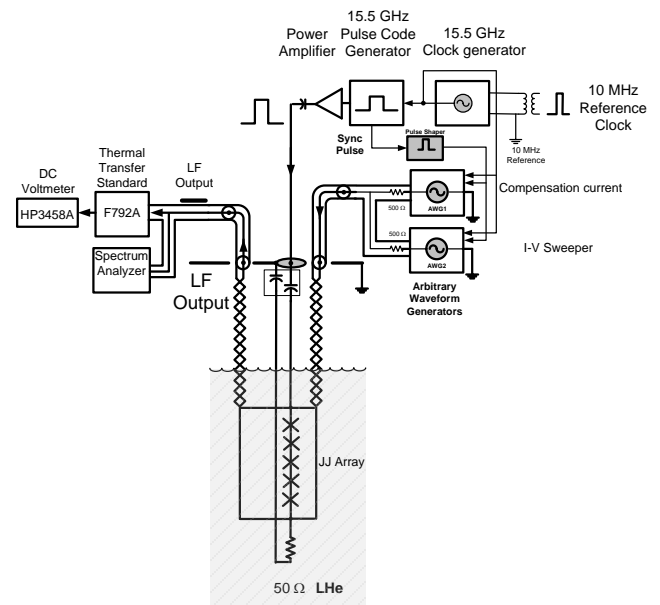


Fig. 1. Simplified circuit diagram of VSL ACJVS.

coupler with a 15-GHz sinewave. A separate analog phase shifter is used to adjust the phase of the sinewave for a proper phase relation between the two signals.

The PCG pattern memory length is  $4 \cdot 10^6$  bits. The lowest frequency which can be synthesized in the described configuration is 2500 Hz.

The compensation current circuit performs the same function as in the VSL system. The output voltage leads are also made of a copper wire twisted pair line. The drooping frequency characteristic of the 6 MHz low pass RC filter (LPF), connected at the output of the cryoprobe, offsets the resonant frequency characteristic of the twisted pair line.

The operation of the system requires adjustment of up to

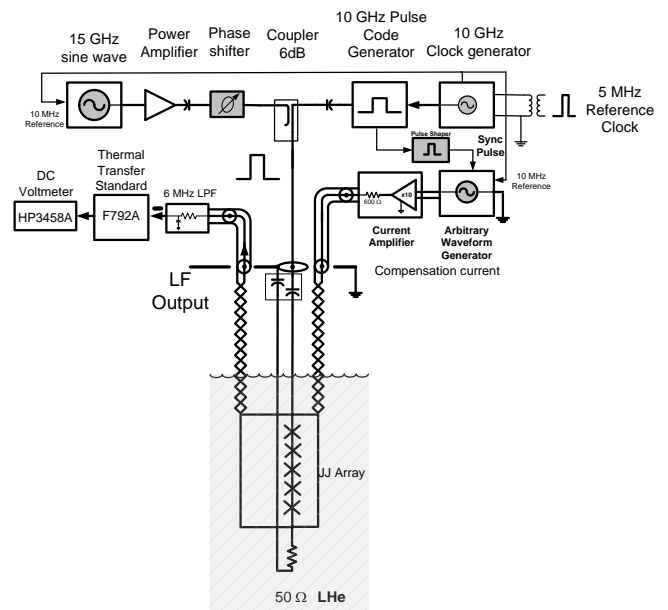


Fig. 2. Simplified circuit diagram of NRC ACJVS

8 parameters. This adjustment is not automated and requires manual intervention of a skilled operator. However, the optimal settings at each voltage/frequency point are stored in the computer memory and recalled for the repeat measurement at the same point. Thus in practice, often only a minor adjustment of the CWG analog phase shifter setting is required after a change in the ACJVS operating point. Once the parameters have been adjusted, the actual calibration of the IUT proceeds under computer control.

Both laboratories use JJ chips manufactured by the NIST as the quantum AC voltage sources. Each chip contains two identical arrays. A single array used as the NRC standard contained 5120 JJs, and could generate up to 110 mV rms AC voltage. The VSL array contained 6400 JJs, with a maximum rms AC voltage up to 138 mV. The chip arrays can be connected in series, to double the output voltage. However, in the reported comparison we limited our measurements to single-array tests.

### 3. DEFINITION OF THE MEASURAND

The two systems were compared by use of an amplifier-aided thermal transfer standard Fluke model 792A as a travelling standard. Determination was made of its AC-DC voltage transfer difference  $\delta$ , the difference between the sinusoidal AC voltage  $V_{AC}$  required for a given output emf and the DC voltage  $V_{DC}$ , which when reversed produces the same mean emf of the transfer standard as the AC voltage, (1).

$$\delta = \frac{V_{AC} - V_{DC}}{V_{DC}} \Big|_{E_{AC} = E_{DC}} \quad (1)$$

where:

$\delta$  is the AC-DC voltage transfer difference in  $\mu\text{V}/\text{V}$ ,  
 $E_{AC}$  is the output emf with an input AC voltage  $V_{AC}$  applied  
 $E_{DC}$  is the mean output emf with an input DC voltage  $V_{DC}$  applied.

### 4 VOLTAGE LEADS ERROR

The output reference plane of the quantum-accurate AC voltage source is located on the array output connections, mounted in the cryoprobe and immersed in liquid helium. It

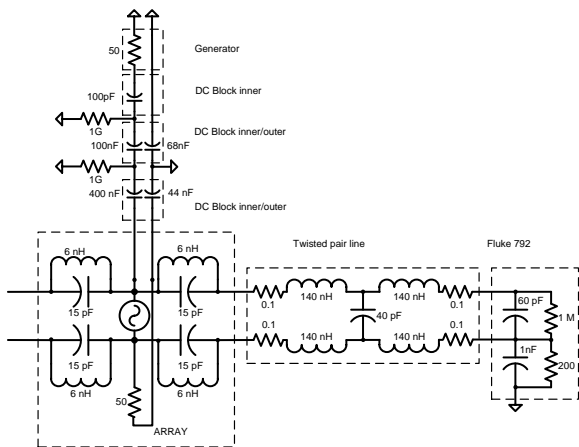


Fig. 3. Part of the ACJVS equivalent circuit used at the VSL to calculate voltage leads error.

is separated from the input reference plane of the IUT by the length of the voltage leads in the cryoprobe, approximately 1.3 m, and any additional cable between the cryoprobe output and the IUT. Voltage drop or rise on these leads is a source of a systematic, frequency dependent error.

The approximate value of the voltage leads error can be calculated from the residual parameters of the leads, [8]. It can be also determined experimentally.

At the VSL, a TSS with a known frequency characteristic of the AC-DC difference, determined by use of a thermal voltage converter, was subsequently calibrated at frequencies between 1 kHz and 1 MHz by the ACJVS. The frequency characteristic of the voltage leads error was calculated as the difference between these two calibration results. The error was closely proportional to the square of the frequency. This behavior was confirmed by calculations on the equivalent circuit. For illustration purposes, Fig. 3 shows part of the equivalent circuit of the ACJVS. Not shown in the figure, but used in the calculations, were the impedances of the leads and the input impedances of the spectrum analyzer and the two AWGs.

Taking advantage of the fact that the error scaled very well with the square of the frequency, the value of the error at lower frequencies was derived from the value of the error determined experimentally at the highest frequency. For example, if the value of the leads error was determined experimentally as equal to  $-10\,000\ \mu\text{V}/\text{V}$  at 1 MHz, at 100 kHz it was calculated as  $-100\ \mu\text{V}/\text{V}$ , [9]. The detailed description of this voltage lead correction procedure will be published in [10].

At the NRC, the voltage leads error was also determined experimentally, by use of an auxiliary working standard, Fig. 4, [11]. The travelling TSS was compared to the auxiliary TSS working standard twice, either directly or at the end of the actual cryoprobe. The reference plane of the first comparison was at the TSS input reference plane and at the JJ array output reference plane during the second comparison. The voltage leads error was calculated as the difference between the results of the two comparisons.

Both laboratories used the value of their experimentally determined systematic error to correct their results.

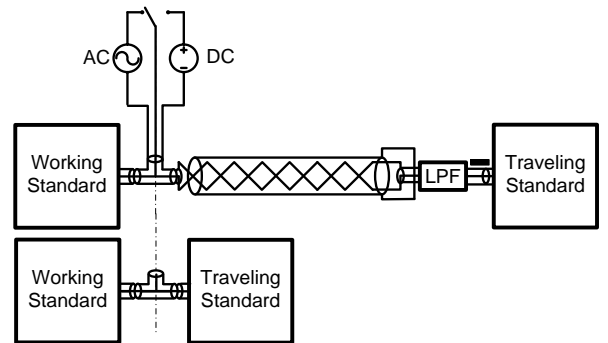


Fig. 4. Simplified schematic of two AC-DC measurements used for experimental determination of the AC-DC difference of voltage leads.

## 5. COMPARISON RESULTS

The results of the comparison are shown in Figs. 5 to 7. Both laboratories measured the travelling standard at 100 mV on the 220 mV range, and at 20 mV and 12 mV on the 22 mV range, at frequencies of (2.5, 5, 10, 20, 50, 70, 100) kHz. Additionally, at the VSL it was measured at 1 kHz and at the NRC it was compared to two thermal converters; at 100 mV to a planar, thin-film, multijunction thermal converter (Fig. 5, TFMJTC-NRC) and at 20 mV and 12 mV to a micropotentiometer (Figs. 6 and 7, Step-down procedure-NRC).

The error bars show the expanded uncertainty,  $k=2$ . The uncertainty budget includes the comparison uncertainty, the voltage leads correction uncertainty, as well as the uncertainty introduced by the LF current compensation. The NRC expanded uncertainty budget included additionally a component reflecting TTS changes with the temperature and power supply batteries.

The expanded uncertainty of  $2.2 \mu\text{V/V}$  at 2.5 kHz for the TFMJTC calibration is relatively large because the converter operates only at 1 % of its maximum output voltage. The expanded uncertainty of the micropotentiometer calibration is (40 to 80)  $\mu\text{V/V}$  over the test voltage and frequency ranges.

At frequencies exceeding approximately 20 kHz, the compensation current voltage drop on the internal inductance of the array has to be taken into consideration as a source of a systematic error, [12]. A voltage of 12 mV was selected because that was the highest voltage at which the ACJVS could operate without the LF current compensation, therefore eliminating this error source.

At the most accurate voltage, 100 mV, the calibration results at both laboratories agreed to better than  $1 \mu\text{V/V}$  up to 10 kHz. At higher frequencies, the differences between the results increase to a few  $\mu\text{V/V}$ , reaching  $19 \mu\text{V/V}$  at 100 kHz. It should be noted that the VSL results agree well with the thermal converter calibrations, whereas at 100 kHz, there is only a weak agreement between the thermal converter and the NRC calibrations. On the other hand, the results at 50 kHz also differ, whereas the NRC result remains closer to the thermal converter calibration. The analysis of these results points to the lead correction determination as the main cause of the disagreement.

At the NRC, the measured lead correction at 2.5 kHz is approximately  $-1.5 \mu\text{V/V}$ . As the frequency increases, it remains at  $(-3 \text{ to } -4) \mu\text{V/V}$  up to 70 kHz, to reach  $+8 \mu\text{V/V}$  at 100 kHz. The relatively flat frequency characteristic of the correction is the result of compensation of the rising characteristic of the twisted-pair leads by the drooping characteristic of the RC low pass filter.

The filter increases the resistance of the leads by the  $50 \Omega$  series resistance, and creates a voltage divider with the frequency dependent input resistance of the TSS ( $2 \text{ M}\Omega$  at 100 kHz). The influence of this divider is corrected by the experimental lead correction, derived as described before, from two measurements at room temperature. In these tests, the direct comparison of the two transfer standards repeated to better than  $1 \mu\text{V/V}$  over 6 months; however, the measurement with the cryoprobe leads included was sensitive (within several  $\mu\text{V/V}$  at 100 kHz) to ground

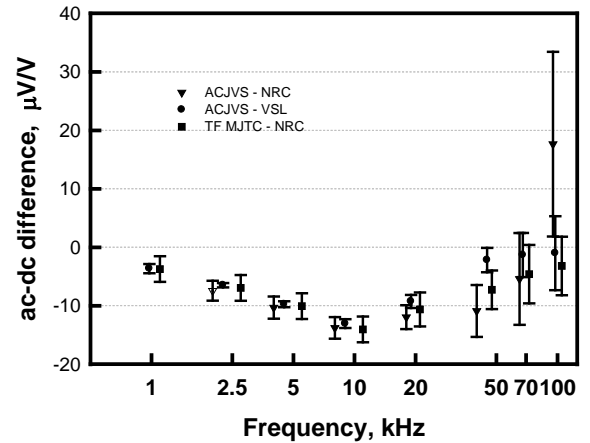


Fig.5. Results of comparison at 100 mV.

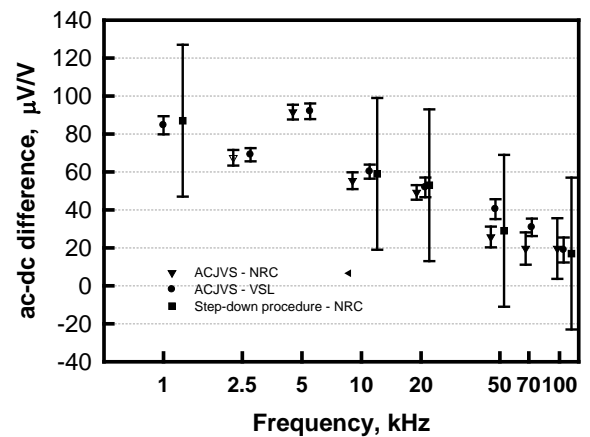


Fig.6. Results of comparison at 20 mV.

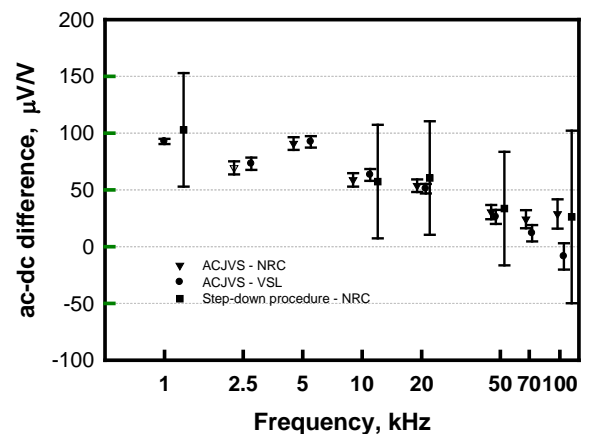


Fig.7. Results of comparison at 12 mV.

connections and the internal impedance of the test AC voltage source. In effect, the bench measurements, using an additional TTS, do not reproduce the same grounding arrangements of the travelling standard as during the ACJVS calibrations.

In contrast to the NRC approach, the VSL does not use any additional filter between the TSS and the cryoprobe output, thus do not introduce any additional resistance to the voltage path, and the correction is calculated from the measurements with the cryoprobe immersed in the liquid helium. Tests conducted at the NIST, [13], as well as at the NRC, indicate that at frequencies above 100 kHz, the AC-DC transfer difference of the voltage leads changes with the level of the lead immersion in the liquid helium. This effect may explain the discussed divergence of the results observed at 100 kHz. Further work is necessary to confirm if this change is due purely to the change in the lead resistance.

The 20 mV and 12 mV results resemble the 100 mV results. As expected, at such a low voltage level the test uncertainties are larger. Nevertheless, the TSS calibrations at both laboratories agree to within 6  $\mu\text{V/V}$  up to 20 kHz. The largest disagreements are, at 100 kHz; 19  $\mu\text{V/V}$  at 20 mV and 29  $\mu\text{V/V}$  at 12 mV. At this frequency point, the experimentally determined lead correction has the largest influence on the NRC test uncertainty.

In spite of the lower voltage level, the agreement at 12 mV is more consistent than at 20 mV. As it was discussed above, at 12 mV both systems operated without the LF compensating current, thus eliminating this error source.

## 6. CONCLUSIONS AND FUTURE WORK

This paper presents results of a bilateral comparison between the NRC, Canada and the VSL, the Netherlands, of two quantum AC Josephson Voltage Standards. In contrast to a previously reported comparison, [14], when very similar ACJVS systems were compared, the systems employed in this comparison use different voltage lead correction mechanisms and different types of pulse generators energizing the arrays. They also differ significantly in the level of automation.

The AC-DC transfer difference of a travelling thermal standard was measured at 100 mV, 20 mV and 12 mV, at frequencies between 2.5 kHz and 100 kHz.

At the most accurate voltage and frequency point, 100 mV at 2.5 kHz, both laboratories agreed to better than 1  $\mu\text{V/V}$ . At 20 mV and 12 mV, the difference was less than 2  $\mu\text{V/V}$  and 6  $\mu\text{V/V}$ , respectively.

At 5 kHz to 70 kHz, the agreement between the two systems remains within the expected uncertainty limits of the travelling standard. However, the difference between the systems at 100 kHz points to a systematic error in determining the voltage lead correction in the NRC system. During the system operation, the leads are partially immersed in liquid helium, while the correction is measured with the voltage leads at the room temperature. A further work is necessary to validate this supposition.

We believe that at low frequency, i.e., below approximately 10 kHz to 20 kHz, the uncertainty of the

comparison was limited only by the inherent characteristics of the travelling standard, such as its short term stability. There was no indication, that any of the hardware or software differences between the systems affected test results.

## ACKNOWLEDGMENTS

The authors want to thank Dr. Sam Benz and the NIST Quantum Voltage Project for providing us with the ACJVS arrays and the collaborative support.

## REFERENCES

- [1] S. P. Benz and C. A. Hamilton, "A Pulse-Driven Programmable Josephson Voltage Standard," *Appl. Phys. Lett.*, vol. 68, no. 22, pp. 3171-3173, May 1996.
- [2] S. P. Benz, P. D. Dresselhaus, C. J. Burroughs and N. F. Bergren, "Precision measurements using a 300 mV Josephson arbitrary waveform synthesizer," *IEEE Trans. Appl. Supercond.*, vol. 17, No. 2, Part 1, pp.864-869, July 2007.
- [3] T. E. Lipe, J. R. Kinard, Y. H. Tang, S. P. Benz, C. J. Burroughs, and P. D. Dresselhaus, "Thermal Voltage Converter Calibrations Using a Quantum AC Standard," *Metrologia*, vol.45, no.3, pp.275-280, June 2008.
- [4] S.P. Benz, P.D. Dresselhaus, A Rufenacht, N.F. Bergren, J.R. Kinard, R.P. Landim, "Progress Toward a 1 V Pulse-Driven AC Josephson Voltage Standard," *IEEE Trans. Inst. Meas.*, vol. 58, No. 4, pp. 838-842, April 2009.
- [5] E. Houtzager, S. P. Benz, and H.E van den Brom, "Operating Margins for a Pulse-Driven Josephson Arbitrary Waveform Synthesizer using a Ternary Bit-Stream Generator," *IEEE Trans. Inst. Meas.*, vol. 58, No. 4, pp. 775-780, April 2009.
- [6] E. Houtzager, H. E. van den Brom, and D. van Woerkom, "Automatic Tuning of the Pulse-Driven AC Josephson Voltage Standard," in *Proc. CPEM 2010*, Daejeon, Korea, June 2010, pp. 185-186.
- [7] S.P. Benz; C.J. Burroughs; T.E. Harvey, C.A. Hamilton, "Operating conditions for a pulse-quantized AC and DC bipolar voltage source," *IEEE Trans. On Applied Superconductivity*, vol. 9, no. 2, pp.3306-3309, June 1999.
- [8] P. S. Filipinski, J. R. Kinard, T. E. Lipe, Y. H. Tang and S. P. Benz, "Correction of Systematic Errors due to Voltage Leads in AC Josephson Voltage Standard," *IEEE Trans. Inst. Meas.*, vol. 58, No. 4, pp. 853-858, April 2009.
- [9] H. E. van den Brom, E. Houtzager, "Minimizing Voltage Lead Corrections for a Pulse-Driven Josephson Voltage Standard," in *Proc. CPEM 2010*, Daejeon, Korea, June 2010, pp. 6-7.
- [10] H. E. van den Brom, E. Houtzager, "Voltage Lead Corrections for a Pulse-Driven Ac Josephson Voltage Standard up to 1 MHz," submitted for publication.
- [11] P. S. Filipinski, M. Boecker, S. P. Benz, and C. J. Burroughs, "Experimental Determination of the Voltage Lead Error in an AC Josephson Voltage Standard," *IEEE Trans. Instrum. Meas.*, vol. 60, July 2011, pp. 2387-2392.
- [12] R. P. Landim, S. P. Benz, P. D. Dresselhaus, and C. J. Burroughs, "Systematic-error signals in the ac Josephson voltage standard: measurement and reduction," *IEEE Trans. Inst. Meas.*, vol. 57, no. 6, pp. 1215-1220, June 2008
- [13] J.R. Kinard, (private communication, NIST, May 2010).
- [14] P. S. Filipinski, J. R. Kinard, T. E. Lipe, and Yi-hua Tang, "An International Comparison of Quantum AC Voltage Standards between NIST and NRC," presented at 2010 NCSL International Workshop and Symposium, Providence, RI, July 2010, paper 1E-1, 9 pages.